Comparison of Simple and Advanced Methods of Analysis in the AISC *Specification* for Fire-Resistant Structural Design

RACHEL CHICCHI and AMIT H. VARMA

ABSTRACT

AISC *Specification* Appendix 4 (AISC, 2016b) provides criteria to aid structural engineers in structural design for fire conditions. It includes an advanced method of analysis and a simple method of analysis. The simple method provides straightforward equations to determine member capacities at elevated temperatures. However, determination of demands on the structure (forces and deformations) due to elevated temperatures is less clear. This paper aims to minimize these gaps in knowledge. A comparison of these methods will be articulated through the analysis of a 10-story office building. The building is a steel structure with perimeter moment frames and a composite floor system that was designed for hazards in Chicago, Illinois. In order to conduct the advanced analyses, a three-dimensional (3D) finite element method building model was developed using ABAQUS (2016). This model can simulate inelastic deformations, instability failures, connection damage at elevated temperatures, and the effect of temperature on strength and stiffness of materials. The simple analyses were conducted using SAP2000 (CSI, 2018), a commercially available structural analysis and design software. A comparison of results from each method of analysis shows that for gravity framing members, the advanced method produced the longest fire-resistance rating. The fire-resistance rating determined from the simple method was more conservative, resulting in a shorter resistance rating. The simple method was also found to be the most conservative approach for the moment-resisting frame members, making it a less desirable method for designing the lateral system for fire than the prescriptive approach. Use of the simple method may be most advantageous for gravity framing applications only and may be overly conservative for considerations of the lateral framing system.

Keywords: fire resistant design, steel, simple method, performance-based design.

INTRODUCTION

Structural design for fire conditions in the United States has traditionally been conducted by architects and fire protection engineers using a prescriptive approach. This approach is based on standard furnace tests of components and assemblies, which do not always correlate well with realistic building behavior. Following the World Trade Center collapse in 2001, structural fire engineering research and design began to move toward a performance-based approach that considers system-level response and design fires specific to each building (occupancy, materials, ventilation, etc.). With this shift, structural engineers have a more active role in the structural design for fire conditions. In an effort to facilitate this shift in responsibility, the American Institute of Steel Construction (AISC) authored and continues to update Appendix 4 of the AISC *Specification* (2016b), which provides guidance on structural design for fire conditions. This appendix includes design guidance for using advanced and simple methods of analysis.

Summary of Structural Design Approaches for Fire

Appendix 4 alludes to three primary methods of analysis or design for fire: the advanced and simple methods of analysis and the prescriptive method for design. The advanced method incorporates several considerations in its analysis. These include strength and stiffness deterioration with increasing temperature, thermal expansions and large deformations, second-order effects, inelasticity, and the ability to simulate all potential limit states, among many others. These analyses are performed in accordance with AISC *Specification* Appendix 1.3.1 (2016b). This modeling approach is often used for large or complex structures with irregularities in stiffness or geometry, though it is becoming an increasingly prevalent approach for analyzing regular buildings as engineers become more competent in designing for fire.

The simple method of analysis is a member-based approach that evaluates member adequacy using load and resistance factor design. It allows the designer to employ reasonable and conservative simplifying assumptions in order to assess member adequacy without the detailed modeling necessary for the advanced method. The simple

Rachel Chicchi, Assistant Professor, Department of Civil and Architectural Engineering and Construction Management, University of Cincinnati, Cincinnati, Ohio. Email: rachel.chicchi@uc.edu (corresponding)

Amit H. Varma, Karl H. Kettelhut Professor in Civil Engineering, Purdue University, West Lafayette, Ind. Email: ahvarma@purdue.edu

Paper No. 2020-13

method approach captures common limit states but does not currently include all potential limit states. For example, local buckling limit states and connection failure modes are not currently considered in Appendix 4. The simple approach also enables the designer to calculate the member design strength at a specific temperature but does not consider the member's behavior over time or evaluate the performance of the structure overall. The design equations for the simple method were primarily based on work by Takagi and Deierlein (2007), which showed close correlation to ECCS (2001) and detailed finite element models that were validated against physical test data.

The prescriptive approach of fire-resistance ratings is based on standard furnace tests of short span members. This approach does not specifically consider building geometries and loadings. The International Building Code (ICC, 2018) specifies the required fire-resistance rating (FRR) based on the ASTM E119 (2015) standard for structural members based on the size, number of stories, use of space, and building importance. This rating is the time (in hours) that an element or system can be exposed to a standard fire before it reaches its critical temperature or approaches collapse under applied loads. A database of successfully tested assemblies is used to determine the fireproofing thickness required on each structural member in order to achieve the necessary fire-resistance rating. The forthcoming 2022 edition of the AISC *Specification* will include more information about the prescriptive method, including design applications.

While the prescriptive approach is used widely in the U.S. building industry due to its simplicity and successful performance history, the standard fire-tested assemblies do not always translate well into real building behavior and can be overly conservative, limiting design capabilities of the structural engineer and architect. The advanced analysis method provides a performance-based approach that allows the design team and the owner to better understand building behavior, including anticipated extent of damage, due to fire hazards. The simple method allows for a comparison of design strength and resistance of individual members that is typically less computationally and labor expensive than the advanced method. These methods provide the potential for optimization of structural framing and flexibility of design.

This paper discusses the analysis of a case study building for a design fire using the simple and advanced methods of analysis. The prescriptive method of design was used to design the case study building and then the adequacy of the design was evaluated and compared with the results of the simple and advanced methods. The primary objectives of this paper are to (1) provide practical recommendations for the implementation of the simple method of analysis using the SAP2000 (CSI, 2018) software and (2) provide a comparison between the results of each method.

BACKGROUND

Existing studies have been performed that apply the advanced analysis method to three-dimensional (3D) steel building finite element models, including Agarwal and Varma (2014), Fischer et al. (2019), Khorasani et al. (2019), and Gernay and Khorasani (2020). These models are capable of capturing all potential limit states, including composite slab behavior, connection failure, and inelastic column buckling. Two-dimensional models or single-compartment 3D models can also be modeled using the advanced method but may not adequately consider slab continuity and boundary conditions that are represented in a full building model.

In addition to previous research studies, the American Society of Civil Engineers (ASCE) published performance-based structural fire design examples that provide additional guidance on structural fire design using ASCE 7-16, Appendix E (ASCE, 2016). This includes design procedures, performance objectives, and recommendations generated by engineers at four different design firms across the United States. Performance objectives are typically determined in coordination with the owner, engineer, and authority having jurisdiction (AHJ). These are metrics of the intended performance of the structure under fire effects. The code-minimum requirement (ASCE, 2016; ICC, 2018) for performance is to maintain structural integrity for a period of time in order to ensure safe and complete evacuation of the building occupants. This period of time is known as the fire-resistance rating. Higher levels of performance may be required such as no collapse throughout the duration of the fire or extending the timeframe of structural integrity (i.e., increasing the fire-resistance rating beyond the code-minimum requirement).

FIRE ANALYSIS AND DESIGN METHODOLOGY

An exemplar case study building will be used to demonstrate the simple and advanced methods of analysis and ultimately compare the results of each method. The fire-resistance rating achieved from each method will be compared as well as the demands determined from each approach. The advanced method provides an indication of the behavior of the system over time through a virtual simulation, while the simple method typically evaluates a design based on the peak demands of the structure. Thus, direct comparison of demands between these two methods is difficult if comparisons are not made at the same point in time. For the purposes of this comparative study, member demands were evaluated at a specific time (at 1 hr). One hour is the building's prescribed fire-resistance rating, and the case study structure was design for this code-minimum requirement.

When performing an analysis and design of a structure under fire, the performance objectives established for that design must be evaluated. If maintaining structural integrity throughout the duration of the fire is a performance objective, then consideration of demands and design strength at all phases of the design fire ought to be considered. Consideration should also be given to the effects of cooling, which could cause contraction (tensile forces) in connections. Connection design using the simple method is beyond the scope of this paper and requires further research and understanding.

Analysis Considerations

Fire Types and Locations

AISC *Specification* Appendix 4 (2016b) indicates that structural members should be designed for a design-basis fire, which is a fire that captures the likely heating conditions within the building based on fuel load densities and compartment characteristics. Appendix 4 specifies three types of design-basis fires: localized, post-flashover compartment, and exterior fires. After ignition and growth of the fire, flashover may occur, which initiates a fully developed, or post-flashover, fire. Localized fires are those that do not cause flashover due to either a lack of fuel or oxygen. These fires typically develop temperatures much lower than post-flashover fires. Post-flashover compartment fires are fully developed fires where the temperature within the compartment is presumed to be homogenous throughout. Compartments are defined as areas within the building that are bounded by fire-rated boundaries that can contain the fire throughout its duration (NFPA, 2020). Exterior fires occur when radiation and flames escape post-flashover compartment fires that could compromise structural members outside of the compartment. Only post-flashover compartment fires are being used in this study. Refer to the Appendix 4 Commentary for additional resources for identifying fire curves for the other fire types.

Engineering judgment must also be used to determine which critical locations within the building to analyze for fire. Areas prone to progressive collapse under fire loading should be considered; this may include members carrying high loads and/or long spans. Consideration should also be given to the likelihood of each fire event; for instance, spaces with equipment that could malfunction and initiate a fire should be considered. Also, areas with high fuel load density should be evaluated, as well as areas less accessible to firefighting measures.

Thermal Gradient

Thermal gradient is the change in internal temperature of a structural member across its length and cross-section. The assumptions regarding the design fire will influence the thermal gradient of the structural member. It was assumed that the fire is post-flashover; thus, a simplified one-zone modeling approach is used, and temperatures are modeled as constant along the length of the member. Localized fires, or those simulated using more realistic fire conditions, may invalidate this simplifying assumption.

Composite beams and steel columns may experience different thermal gradients along their cross section. The bottom flange of a composite beam is typically exposed to a fire from all sides while the top flange is insulated by the concrete slab on metal deck it connects to. This creates a higher internal temperature in the bottom flange of the beam than the top flange, creating a nonuniform thermal gradient in composite beams. The simple method accounts for this by applying a 25% reduction in steel temperature at the top flange of the cross section relative to the remainder of the cross section. When using the advanced method, the temperature gradient is typically determined by conducting heat transfer analyses to determine temperatures at different locations along the cross section.

In this study, it was assumed for simplicity that the columns were subjected to uniform heating from all sides. In design, this assumption should be carefully considered. The layout of the compartments and the location of the columns within the compartment or at the exterior of the compartment would influence the fire exposure assumptions for the columns. For instance, for a column located in the center of a compartment exposed to a post-flashover fire, uniform fire loading is a reasonable assumption. However, if the column is located at the edge of a compartment where there is a potential for one side (or corner) of the column to be exposed to the fire and other sides to not be, a nonuniform fire-loading scenario may want to be employed.

Nonuniform heating on gravity columns was studied by Agarwal et al. (2014) and Choe et al. (2016). They found that slender columns with heavy loading experienced premature elastic buckling due to the thermal gradient; however, most nonslender columns were minimally affected by the thermal gradient. For these reasons, the columns in this study were assumed to experience a uniform thermal gradient.

Fire Load Combination

Appendix 4 specifies the following load combination to be used for fire analyses. This load combination also corresponds to the load combination for extraordinary events in ASCE/SEI 7 (2016).

$$12D + A_T + 0.5L + 0.2S \quad (1)$$

where D is the dead load, L is the live load, and S is the snow load. The variable A_T is defined as the nominal forces and deformations due to the design-basis fire, which can be

simulated directly through the analysis. A dead load factor of 0.9 may also be used in Equation 1 in lieu of the 1.2 factor in situations where the dead load helps stabilize the structure. Note that it may be preferable to use roof live load instead of snow load for structural fire design since the probability of snow load concurrently with fire is low. Live load reduction (LLR) per ASCE/SEI 7 was not considered in the presented results. However, live load reduction, which accounts for the reduced likelihood of the full live load acting on the structure, can be helpful in reducing the demands on the structure. Incorporating live load reduction may be especially beneficial for evaluating column designs. This load combination was used for both the simple and advanced methods of analysis.

Case Study Building

The case study structure is a 10-story office building designed to comply with U.S. building codes and standards: IBC (ICC, 2018), ASCE/SEI 7 (2016), and the AISC *Specification* (2016b). The structure was designed for hazard levels in Chicago, Illinois. It is a three-bay by five-bay structure, with each bay measuring 25 ft (7.63 m) × 25 ft (7.63 m). Each story height is 12 ft (3.66 m). The structure is a traditional steel-framed building with a partially composite floor system. The lateral system is a perimeter moment frame system using ordinary moment frames. Refer to Figure 1 for a typical framing plan. Triangles at columns indicate moment connections.

Preliminary Design

The building was designed for a dead load of 65 pounds per square foot (psf) and a live load of 50 psf. The composite floor slab is a 3-in., 20-gauge (75-mm) composite deck with 2½-in. (65-mm) lightweight concrete topping. The gravity beams are W14×22 and the gravity girders are W18×35. For simplicity, the gravity framing for the roof is the same as the typical floors. The moment frame design was controlled by a wind drift limit of $L/400$, where L is the building height. Table 1 shows the moment frame and gravity column member sizes.

The minimum fireproofing required for each member was determined using the prescriptive method of design. The case study office building is classified as building occupancy B per IBC, which corresponds to a Type IB building. Type IB buildings require a 2-hr FRR on all framing members; however, if proper control valves and initiating devices are used in conjunction with the sprinkler system, then the building can be reduced to Type IIA per IBC, Section 403, which requires only a 1-hr FRR for all structural members. The case study building was designed for a 1-hr FRR per Type IIA construction.

Spray-applied fire-resistive material (SFRM) was selected to protect the steel members and achieve the necessary 1-hr FRR. Fireproofing thickness, d_p, for each structural member was determined based on fire tests conducted by Underwriters Laboratory (UL) (2018). These tests consist of a limited number of individual components and assemblies

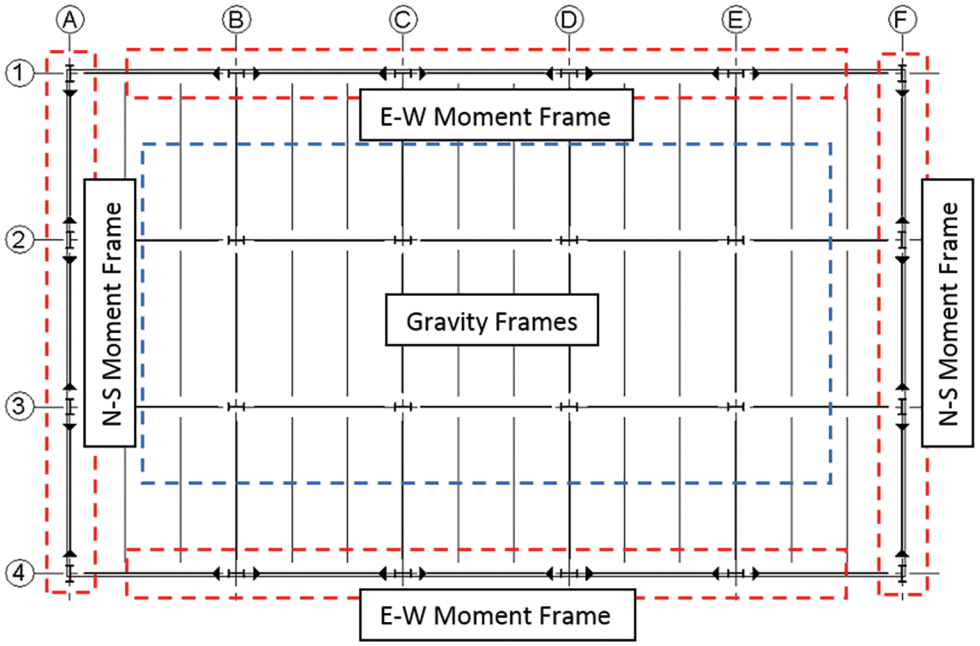

Fig. 1. Case study building framing plan.

Table 1. Member Sizes Used in Case Study Building					
Story	**N-S MF Beams**	**N-S MF Columns**	**E-W MF Girders**	**E-W MF Columns**	**Gravity Columns**
9–10	W18×50	W14×53	W18×35	W12×45	W8×24
7–8	W21×83	W14×90	W18×50	W14×53	W8×40
5–6	W21×93	W14×109	W18×60	W14×99	W12×58
3–4	W21×111	W14×159	W18×71	W14×145	W14×74
1–2	W27×217	W14×311	W21×132	W14×283	W14×90

Table 2. SFRM Thicknesses per Prescriptive Approach			
	Member Size	**UL Assembly**	**Thickness, d_p, in. (mm)**
Beams	W14×22	D902	1⅛ (18)
	W18×35	D902	9⁄16 (15)
	W18×60	D902	½ (13)
	W21×93	D902	⅜ (10)
Columns	W12×58	X772	1⅛ (18)
	W14×99	X772	9⁄16 (15)
	W14×109	X772	9⁄16 (15)

subjected to furnace tests per ASTM E119 (2015). Ruddy et al. (2003) provide guidance to designers on how to use fire test results to determine fireproofing thicknesses.

Heat transfer is a function of both the density and surface area of a member. Therefore, wide flange members are categorized by a W/D value, where W is the weight per linear foot and D is the perimeter of the member cross section that is exposed to the fire. Thickness adjustment equations provided in UL are used to convert the fireproofing thickness of the tested beam or column to the necessary thickness of the member being designed. Table 2 summarizes the member sizes, UL assembly designations, and SFRM thicknesses determined for the structural members analyzed in this project. Thicknesses were rounded to the nearest 1⁄16 in. The composite deck is not fire protected, as it can already achieve the fire-resistance rating without fireproofing per UL Design D904.

Fire Hazard Selection

The temperature versus time profile of the design-basis fire should account for fuel load, compartment dimensions, thermal characteristics of the compartment (i.e., walls and ceiling), and ventilation of the space (both natural and mechanical). Standard fire curves such as ASTM E119 (2015), ISO 834 (2015), and Eurocode 1991-1-2 (CEN, 2002) are commonly used to define fire curves. As an alternative to using standard fire curves, the designer may choose to conduct computational fluid dynamics (CFD) or physical fire tests. The National Institute of Standards and Technology (NIST) also provides the Fire Dynamics Simulator (FDS), which is a CFD program for simulating fire conditions (NIST, 2013). Appendix 4 does not provide specific guidance on how to select the time-temperature fire curve but provides references to assist in selection.

The Eurocode (CEN, 2002) parametric time-temperature approach for determining fire time-temperature curves may be preferable to the other standards because of its simplicity, the ability to modify the curve based on specific building parameters, and the fact that it includes both a heating and cooling portion. This cooling phase can be important as it results in thermal contraction, which can produce large tensile forces and fail connections. These parametric curves assume that the compartment contains a fully developed fire with uniform temperature through the space. These curves are limited to compartments with rectangular enclosures, floor areas less than 500 m^2, ceiling heights less than 4 m, and no ceiling openings. Eurocode time-temperature curves are calculated using three primary variables: the thermal inertia of the enclosure, b, $(J/m^2s^{½}K)$; opening factor, O, $(m^{½})$; and fire load density, $q_{t,d}$, (mJ/m^2). Eurocode provides guidance on the determination of these values based on the building use, geometry, ventilation, etc. Thermal inertia incorporates the density, specific heat, and thermal conductivity of the walls, ceiling, and floor of the compartment. The opening factor is calculated based on the ratio of opening area to wall area. The fire load density is based on the use of the space (i.e., the combustible materials within the space), as well as the fire-fighting measures and active fire suppression systems.

Figure 2 shows the Eurocode parametric time-temperature curve that was used for this study, denoted in the figure as EN 1991-1-2. The parameters that generated this curve are $b = 1000$ J/m^{2}s^{½}K, $O = 0.032$ m^{½}, $q_{t,d} = 1600$ mJ/m^2. These parameters were chosen because the corresponding Eurocode curve approximately follows the ASTM E119 and ISO 834 curves for 1 hr before beginning the cooling phase. The prescriptive approach is based on physical testing using ASTM E119 or ISO 834 fire curves. By selecting a design fire that matches these curves, a reasonable comparison can be made between the prescriptive approach and the results of the simple and advanced analyses.

The design engineer should use engineering judgment and consult with the owner and the AHJ when selecting appropriate design fires for each building and compartment. For instance, instead of analyzing only one fire scenario, the designer may choose to analyze an array of fire curves to account for a broader range of exposures. Additionally, compartment fires are likely to vary among different areas of the building based on openings (i.e., more openings likely at exterior or corner compartments than interior compartments), changes in fuel load densities based on the use of the space, and thermal properties of the compartment.

Fire Location Selection

For the purposes of this study, only compartment fires were studied with the presumption that each bay of the structure is an individual compartment. The fifth story (mid-height of the structure) was analyzed because it is beyond the reach of firefighting ladders and hoses, and the columns are still exposed to large axial forces. Three compartments were analyzed and are classified as compartments 5A (corner compartment), 5B (exterior compartment), and 5C (interior compartment), as shown in Figure 3(a). Member sizes for compartment 5A are shown in Figure 3(b), as this is the compartment that will be presented in detail. Results from compartments 5B and 5C are provided in the Appendix.

SUMMARY OF ANALYSES

For the advanced method of analysis, a three-dimensional finite element model of the case-study structure was developed using ABAQUS (2016), a commercially available finite element method (FEM) software. This nonlinear, inelastic model can simulate inelastic deformations, instability failures, connection damage at elevated temperatures, and the effect of temperature on material strength and stiffness. The modeling approach was adapted from Agarwal (2011). Heat transfer analyses were performed in order to determine internal temperatures of structural members throughout their cross section. Temperature gradients were applied to the model in 5-min increments.

The simple method of analysis outlined in Appendix 4 allows the structural designer to consider and design for thermal loads within the structure, much in the same way that other loads (i.e., gravity, wind, seismic, etc.) are evaluated. The demands and capacities of individual structural members are determined in order to adequately design the structure using load and resistance factor design (LRFD). This procedure will be applied to the case study building and explained in subsequent sections.

Even within the simple procedure, two different approaches can be used. The first approach is an individual member approach that evaluates individual members in isolation. This approach assumes that the load effects (demands or required strengths) can be assumed to be the same as the ambient conditions. This simplifying assumption should be used with caution and only with proper engineering judgment. It can typically be reasonably applied to regular

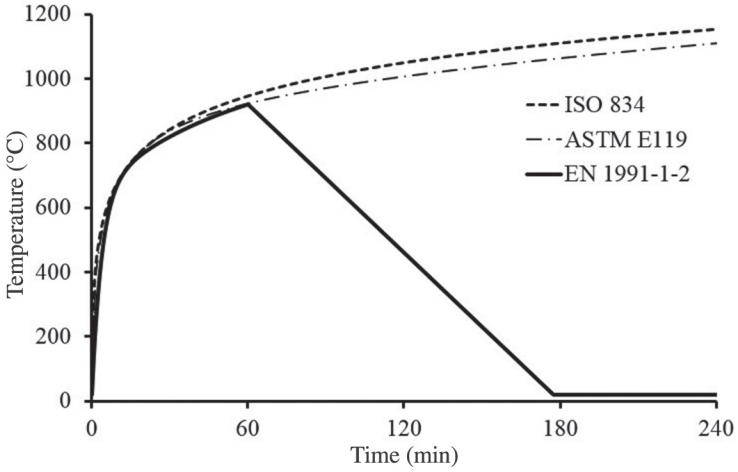

Fig. 2. Fire time-temperature curves.

gravity frames. Alternatively, the second approach evaluates frame behavior. With this approach, stiffness reductions, thermal deformations, and appropriate boundary conditions must be considered. This frame-level approach may be more appropriate for irregular frames with discontinuities. The frame-level approach for the simple method was used throughout this paper using the analysis software, SAP2000.

Modeling Approach

Elements and Connections

Advanced Method

The beams and columns were modeled using two-node beam elements, which approximate 3D solid elements using Timoshenko beam theory. The composite slab was a four-node, reduced integration shell element. Only the concrete above the flutes (2½ in. thick) was modeled for conservatism and simplicity. ABAQUS contains a built-in embedded rebar option that was used to represent the metal deck. The area of rebar matches the area of metal deck applied only in the strong direction of the deck and was located at the centroid of the shell element. There is no reinforcing applied in the weak direction of the deck. The shear studs, which transfer forces between the slab and beams, were modeled using rigid connectors. A schematic of the modeling approach is shown in Figure 4.

The moment frame connections were modeled as rigid connectors. This simplification was made due to work by Yang et al. (2009), which found through experimental testing that the tested moment connections maintained design strength up to 650°C and with only a 25% reduction in stiffness. The shear tab (gravity) connections in the building were modeled using equivalent wire connector elements that capture the axial force-axial

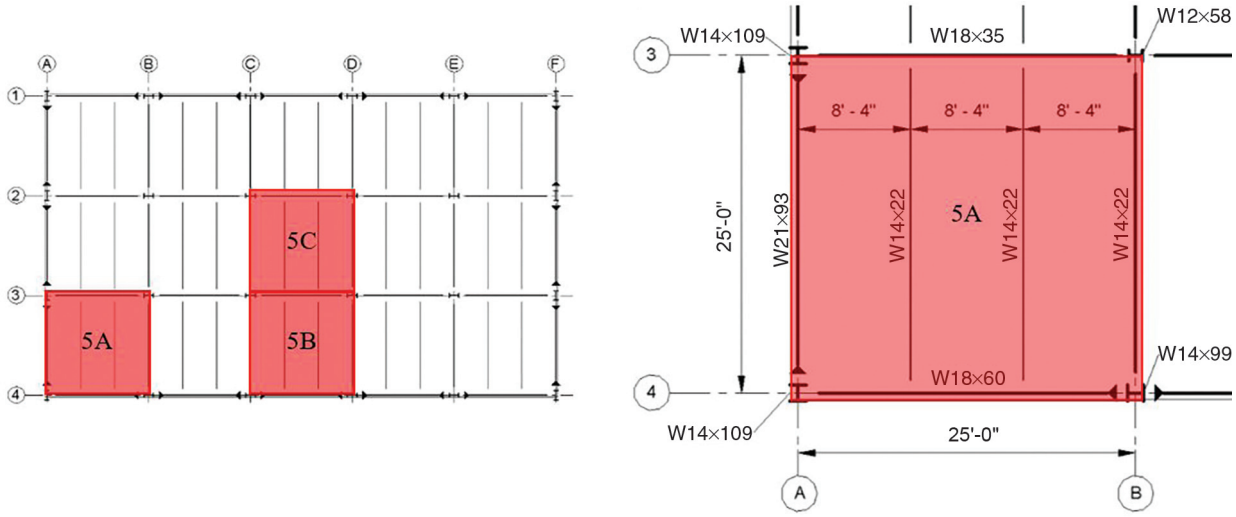

(a) Compartment fire locations *(b) Member sizes in compartment 5A*

Fig. 3. Layout of compartment fires and member sizes.

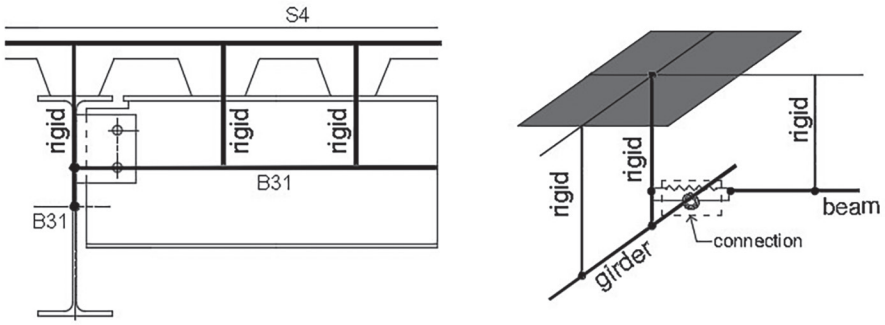

Fig. 4. Schematic of modeling approach for composite floor system (Agarwal and Varma, 2014).

Table 3. Individual Member Analysis—End Restraints

	(a)	(b)	(c)
W14×22 member	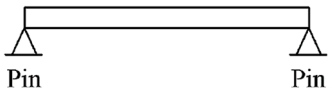	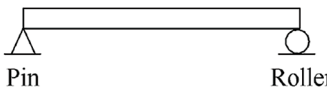	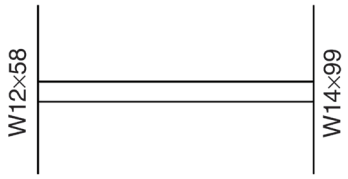
Axial load diagram	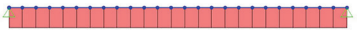		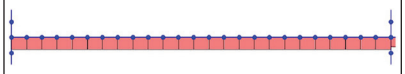
Axial load, *F*	310 kips	0 kips	59 kips

displacement-moment-rotation-temperature behavior, based on work by Sarraj (2007) and Agarwal and Varma (2014). It may be especially important to model this behavior so that fracture during the cooling phase, when the steel contracts, can be captured. Fischer et al. (2021) provide a research review of simple shear connection research conducted by a vast number of researchers.

Simple Method

Structural steel elements, such as beams and columns, inherently want to expand when exposed to elevated temperatures. This expansion may be partially resisted by the adjacent members framing into the heated element. The stiffness of the adjacent members and the rigidity of the connections influence the level of restraint to which the heated member is subjected. Therefore, if following a frame-level analysis approach, it is imperative that these conditions are modeled in order to accurately simulate member behavior. This is illustrated in Table 3 for a W14×22 beam. This member is 25 ft (300 in.) long and was modeled with different end constraints using SAP2000, a commercially available structural analysis and design software. Using idealized pin constraints at both ends of the heated member induced unrealistically high axial loads [Table 3(a)]. The pin restraints do not permit any movement of the member ends, resulting in very high reactions at these supports. The axial force, F, induced on the beam due to a temperature of 1306°F was found to be 310 kips using SAP2000. This value can be verified using Equation 2, which is based on the theory of thermal expansion:

$$F = EA\alpha\Delta T \tag{2}$$

where E is the modulus of elasticity (4,692 ksi due to the elevated temperature), A is the cross-sectional area of the member (6.49 in.^{2}), α is the coefficient of thermal expansion (7.8×10^{-6}/°F), and ΔT is elevated temperature (1,306°F).

If a roller is used to replace one of the pins, then all thermally induced axial loads disappear because there is no restraint to prevent expansion [Table 3(b)]. Because the structural response to fire is highly interdependent on system behavior, analyzing members as individual components in isolation is not recommended. Instead, modeling of the structural system is suggested because it provides reasonable modeling of end restraints. Table 3(c) shows the thermally induced axial load for the simply supported beam framing into W12×58 and W14×99 columns oriented in their weak direction. The resulting axial load of 59 kips demonstrates that the adjacent framing members provide some level of restraint against thermal expansion. If the columns were also exposed to elevated temperatures, the axial load in the W14×22 beam would be influenced by the reductions in column stiffness. Approach (c) is the preferred approach for modeling because Approach (a) with pin-pin constraints results in overly conservative loads and Approach (b) with pin-roller constraints does not account for any axial loads.

As an alternative approach to Approach (c), individual members could be modeled in isolation using spring constraints, but this would require determination of simplified spring constants that represent system behavior. It was decided that modeling the structural system would be simpler. In some cases, such as infill beams with regular, orthogonal framing, Approach (b) may be deemed a reasonable simplifying assumption. Engineer judgment is needed in order to make such simplifications.

SAP2000 was used to model the primary steel members (beams and columns) of the case study building and determine member demands. The steel building was modeled in 3D as shown in Figure 5. Member capacities were calculated by hand using the Appendix 4 equations in Section 4.2.4d. The models include geometric nonlinear (P-delta) effects and linearly elastic material properties. In addition to the load combination described in Equation 1, global stability of the structure should be assessed. This was achieved through notional loads that are 0.2% of the gravity load, which are used to represent the allowable

out of plumb value of $L/500$ (where L is the height of the structure) in accordance with the AISC *Code of Standard Practice* (2016a). The direct analysis method, explained in AISC *Specification* Section C2.2 (2016b), was used. This includes a 20% reduction of stiffness (*EI* and *EA*) for all members. For simplicity, τ_b was set equal to 1.0, and 0.1% of additional gravity loading was applied as notional loads in accordance with AISC *Specification* Section C2.3(c). In lieu of using notional loads, initial imperfections can be directly modeled in accordance with AISC *Specification* Section C2.2a.

For simplicity, only the steel framing was modeled and the composite slab was omitted. Designers may choose to include the composite slab in the model, but then heat transfer would also need to be conducted on the concrete slab. Additionally, SAP2000 does not have a built-in composite slab shell element, so engineering judgment would need to be made in order to appropriately model the slab using a simplified shell element with shell offsets, body constraints, or links. Main and Sadek of NIST (2013) recommend a weak strip–strong strip approach that can be used with relative ease of modeling.

Material Models

Advanced Method

The Eurocode (CEN, 2002) material models were used for steel and concrete, including thermal properties of conductivity, specific heat, and coefficient of thermal expansion. These codes provide stress-strain relationships at elevated temperatures. These relationships will also be included in the 2022 AISC *Specification*. Isotropic hardening was incorporated into the steel model. The material model for concrete is based on two failure mechanisms: tensile

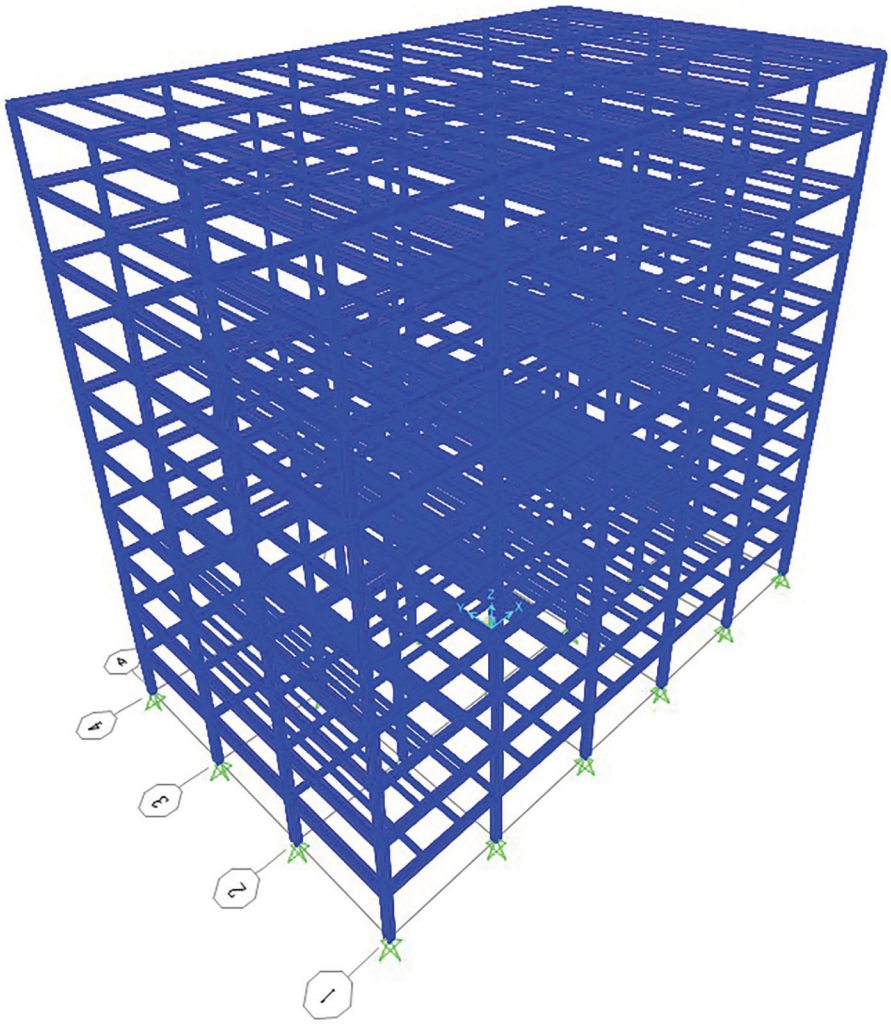

Fig. 5. SAP2000 building model.

Table 4. Steel Temperatures and Material Properties for the Simple Method						
	Member Size	Steel Temperature, °F (°C)	$k_E = E(T)/E$[a]	$E(T)$,[b] ksi	$k_Y = F_y(T)/F_y$[a]	$F_y(T)$,[b] ksi
Beams	W14×22	1150 (621)	0.29	8,382	0.43	21.5
	W18×35	1128 (609)	0.37	10,866	0.48	24.0
	W18×60	993 (534)	0.50	11,513	0.67	33.5
	W21×93	977 (525)	0.51	14,821	0.69	34.6
Columns	W12×58	898 (481)	0.58	16,895	0.80	40.2
	W14×99	869 (465)	0.61	17,654	0.85	42.2
	W14×109	826 (441)	0.65	18,772	0.91	45.2

[a] k_E and k_y are determined based on Appendix 4, Table 4.2.1.
[b] $E(T)$ and $F_y(T)$ are calculated based on the relationship of $E(T)/E$ defined by k_e and $F_y(T)/F_y$ defined by k_y.

cracking (using concrete damaged plasticity) and compressive crushing. The concrete material model was based on siliceous aggregates and lightweight concrete.

Simple Method

AISC *Specification* Appendix 4, Section 4.2.4d, provides equations for calculating the nominal strength of members at elevated temperatures due to tension, compression, flexure, and shear. These equations reference the strength equations in the AISC *Specification* for ambient conditions, with modifications to material properties in order to analyze and design for elevated temperatures.

AISC *Specification* Appendix 4, Section 4.2.3, consists of tables (Table A-4.2.1 through Table A-4.2.3) that contain retention factors. These factors are used to modify material properties at ambient conditions to represent material properties at elevated conditions. The ambient values used were based on ASTM A992 steel: F_y = 50 ksi, F_u= 65 ksi, and E = 29,000 ksi. Table 4 shows calculated material properties based on the retention factors interpolated from the Appendix 4 tables. The coefficient of thermal expansion, α, is $7.8 \times 10^{-6}/°F$ ($1.4 \times 10^{-5}/°C$) for structural steel at elevated temperatures, as provided in Appendix 4.

Heat Transfer

Advanced Method

Before member temperatures can be assigned to the FEM building model, heat transfer analyses must be conducted. ABAQUS was used to conduct 2D heat transfer analyses of each structural member subjected to elevated temperatures. The Eurocode time-temperature curves assume that the compartment fire is a fully developed fire with uniform temperature throughout the compartment, so temperature is uniform along the length of the structural member and, therefore, there is no need to use 3D heat transfer. The cross section of each member was modeled as a 2D part with the fireproofing at the thickness determined from the prescriptive method. In order to compare with the simple method of analysis that requires a uniform temperature gradient, this same assumption of uniform temperature was applied to columns in the advanced model. Beams were modeled with the composite slab. Thermal properties (specific heat, thermal conductivity, and coefficient of thermal expansion) for steel and concrete were taken from Eurocode. Thermal properties of fireproofing were based on Design Guide 19, *Fire Resistance of Structural Steel Framing* (Ruddy et al., 2003) recommendations: specific heat of 0.18 Btu/lb °F (754 J/kg °C), thermal conductivity of 0.0013 Btu/hr ft °F (0.135 W/m °C), and mass density of 18.3 pcf (293 kg/m^3). ECCS (1995) also provides thermal properties of fireproofing, but these values were based on ambient-temperature properties. Guidance on thermal properties of fireproofing at elevated temperatures can be found in Carino et al. (2005) and Kodur and Shakya (2013). SFRM properties are temperature dependent, so incorporating temperature-dependent SFRM properties in advanced analyses may be more appropriate. For the purpose of comparison with the simple method, the average values provided in AISC Design Guide 19 were used in this study.

A film subroutine, which includes radiation and convective effects, was used to conduct the heat transfer analyses per Cedeno et al. (2008). The program conducts thermal transfer of heat from the fire to the structural component in 2D across the member cross section. Internal temperatures are then recorded at integration points defined by ABAQUS for standard cross-sectional beam elements. As shown in Figure 6, five integration points (one at each flange edge and one in the web midspan) are used for the wide-flange cross section. ABAQUS linearly interpolates the temperatures between the beam flanges and parabolically interpolates

along the web. Five integration points are also used for the slab (shell element), resulting in a linear interpolation of temperatures. Because only the concrete above the deck flutes was modeled in the building model, temperatures in the slab were recorded at points uniformly distributed across that portion of the slab. Secondary beams were analyzed using the cross section shown in Figure 6, which considered the locations along the beam where the deck flutes are connected to the top surface of the top flange. Designers may want to also evaluate the locations along the beam where the top surface of the beam is not directly attached to the deck flutes. Girders were analyzed in a heat transfer model that included the deck flute geometry.

Figure 7 shows how a W14×22 composite beam subjected to the design-basis fire varies in temperature over time. The steel reaches much higher temperatures than the slab. Additionally, the top flange of the member reaches lower temperatures than the web and bottom flange due to the presence of the slab acting to insulate the top flange. The time-temperature response of the interior gravity column is shown in Figure 8.

Simple Method

The AISC *Specification* Appendix 4 Commentary outlines a simple approach for heat transfer known as lumped heat capacity analysis. This one-dimensional analysis can be used to calculate the internal temperature of steel members assuming a uniform temperature distribution of the fire. For each member subjected to the compartment fire, internal steel temperatures were determined using the equation for protected steel members assuming that Appendix 4, Commentary Equation C-A-4-5, is satisfied:

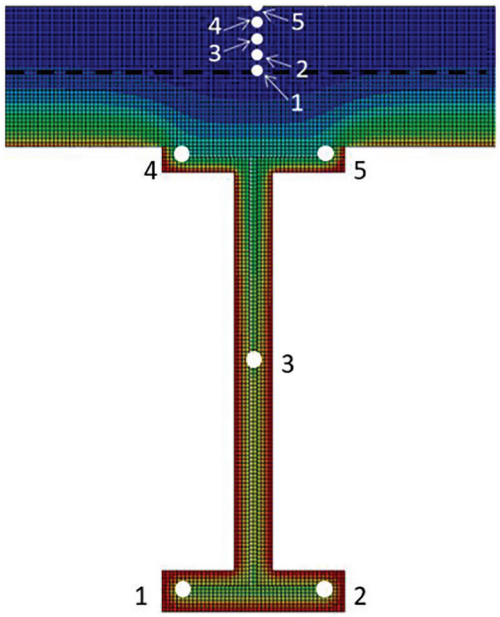

Fig. 6. Temperature gradation and integration points at composite slab with beam directly below.

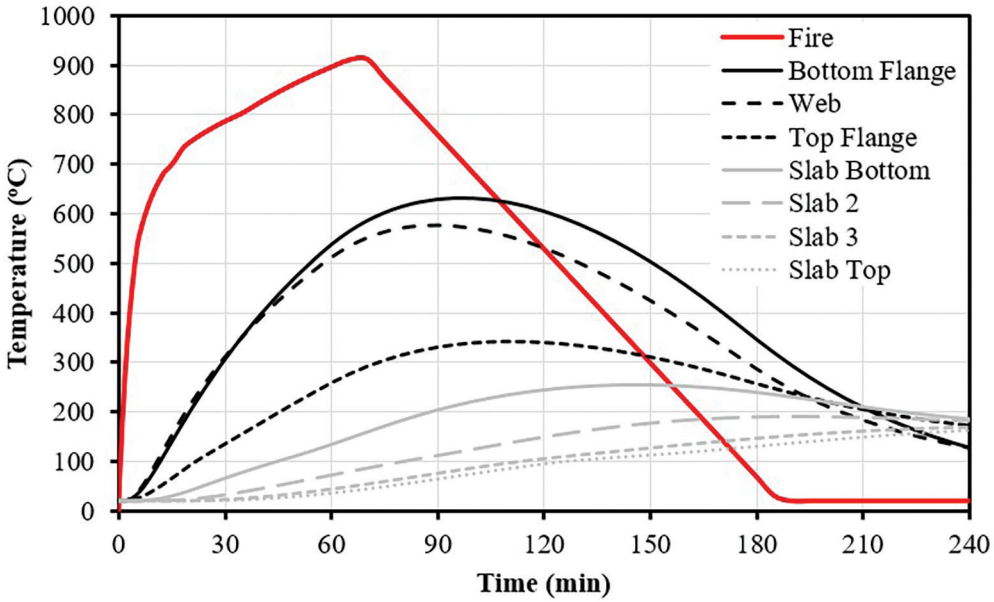

Fig. 7. Time-temperature response of W14×22 composite beam with 1-hr FRR fire protection exposed to fire.

$$\Delta T_s = \frac{k_p}{c_s d_p \frac{W}{D}} (T_F - T_s) \Delta t \quad (3)$$

where ΔT_s is the change in steel temperature, T_F is the temperature of the fire, and T_s is the temperature of the steel. The time step, Δt, should not exceed 5 s. The thermal properties of SFRM vary by manufacturer. In lieu of manufacturer data, thermal properties were taken from Design Guide 19. The values of density, ρ_p, specific heat, c_p, and thermal conductivity, k_p, used for fireproofing were the same values used in the advanced method. The specific heat of steel, c_s, varied with temperature and the values were taken from the Eurocode.

The Appendix 4 Commentary also provides a heat transfer equation for cases with unprotected steel, as well as an alternative equation for protected steel when the thermal capacity of the insulation is comparable to the steel thermal capacity. The fireproofing thicknesses, d_p, determined from the prescriptive method, were used in the heat transfer calculation in order to directly compare the prescriptive and simple methods to one another. The resulting time-temperature curve for a W12×58 column is shown in Figure 8. The Simple curve is the uniform temperature of the W12×58 calculated using the lumped heat capacity equation. The Advanced curve shows the temperature determined through computational heat transfer analyses for the advanced method. This temperature was recorded at the tip of the column flange. This shows a reasonable relationship between the simple and advanced methods of heat transfer analysis.

Table 5 provides the internal temperatures calculated using the lumped heat capacity analysis for each of the members subjected to compartment fires after 1 hr of heating and at the peak temperature. Peak temperatures will likely be used for analysis with the simple method, but this study will record temperatures at 1 hr in order to compare the simple and advanced methods. Table 6 provides a summary of the internal steel temperatures recorded at 1 hr from the ABAQUS heat transfer analyses versus the simple lumped heat transfer method. Temperatures for the bottom flange, web, and top flange are recorded at locations 1, 3, and 4 in Figure 6, respectively. Temperatures resulting from the simple method tend to be conservatively higher than the ABAQUS results. The bottom flange temperatures in both methods are reasonably comparable.

Thermal Loading

Advanced Method

Temperatures determined from the heat transfer model were recorded at the five integration points for the wide-flange members, which were modeled as beam elements. Five points were also recorded along the depth of the slab, which was modeled as a shell element. These temperatures were

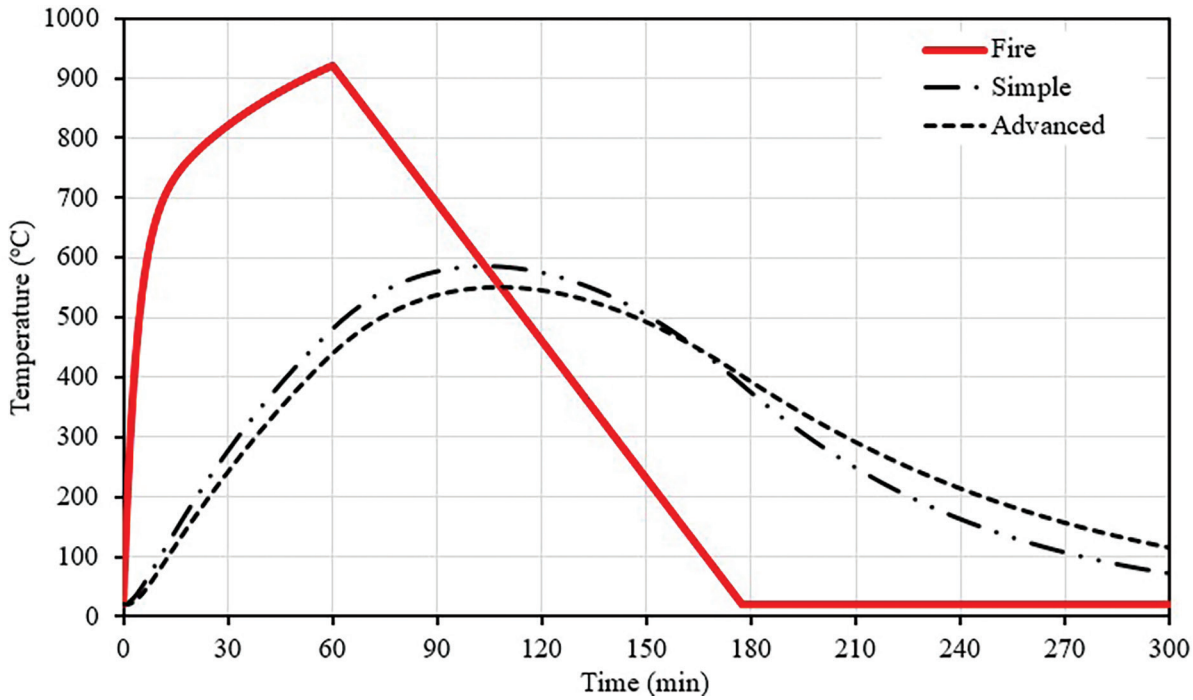

Fig. 8. Results of lumped heat capacity analysis for W12×58 column.

Table 5. Member Temperatures Determined from Lumped Heat Capacity Analysis			
	Member Size	T_s at 60 Min °F (°C)	T_s Max °F (°C)
Beams	W14×22	1150 (621)	1276 (691)
	W18×35	1128 (609)	1261 (683)
	W18×60	993 (534)	1160 (627)
	W21×93	977 (525)	1148 (620)
Columns	W12×58	898 (481)	1087 (586)
	W14×99	869 (465)	1063 (573)
	W14×109	826 (441)	1027 (553)

Table 6. Steel Temperatures in Structural Members at 60 Min. (Simple Method vs. ABAQUS)					
		Steel Temperature, °F (°C) at 60 Min			
			ABAQUS		
	Member Size	Simple	Bottom Flange	Web	Top Flange
Beams	W14×22	1150 (621)	999 (537)	953 (512)	496 (258)
	W18×35	1128 (609)	1040 (578)	1049 (583)	511 (284)
	W18×60	993 (534)	914 (508)	945 (525)	481 (267)
	W21×93	977 (525)	913 (507)	986 (530)	508 (282)
Columns	W12×58	898 (481)	792 (440)	851 (473)	792 (440)
	W14×99	869 (465)	817 (436)	763 (406)	817 (436)
	W14×109	826 (441)	759 (404)	707 (375)	759 (404)

recorded at 5-min intervals and input into the ABAQUS structural model as internal temperatures of the structural members within the compartment. Because the material models implemented in ABAQUS incorporated the stress-strain behavior and thermal elongation at elevated temperatures, these temperatures applied to the model resulted in member forces and deformations due to fire.

Simple Method

Temperature effects on member forces and deformations were accounted for by assigning member temperatures, modified steel mechanical properties at elevated temperatures, and coefficient of expansion values. For each fire scenario, three models were created to compare the effect of changing parameters on the member forces that were observed. These models, which all include notional loads and second-order effects, are:

Case 1: Model only gravity loads ($1.2D + 0.5L$).

Case 2: Model Case 1 plus member temperatures and the coefficient of thermal expansion.

Case 3: Model Case 2 plus modulus of elasticity reductions for members exposed to fire.

When evaluating the forces in the beams due to elevated temperatures, the axial loads were very high when assigning the lumped steel temperature across the entire cross section. With a uniform temperature throughout the cross section, these forces acted only axially and did not produce any thermally induced moments that would be expected in reality. The composite slab insulates the top flange of the beam, which results in lower temperatures at that location. Appendix 4, Section 4.2.4d(d), allows for a 25% reduction in steel temperature at the top flange of the cross section. The reduced temperature can be used for the top half of the beam, as shown in Figure 9(a). This simple method of analysis conservatively produces steel temperatures greater than the advanced analyses, as was demonstrated in Table 6.

Temperature effects can be assigned to the member cross sections using SAP2000. The software currently permits a constant temperature over the cross section as well as linear temperature gradients along the depth and width of the cross section. The temperature profile shown in Figure 9(a) cannot currently be applied in SAP2000. Instead, a constant temperature, T_{equiv}, and a linear gradient were combined to produce the temperature profile in Figure 9(b). The constant temperature was applied to the SAP2000 model in order to produce an equivalent axial load as the profile

in Figure 9(a) (i.e., area times change in temperature are equal), along with a linear gradient. This approach produced slightly higher thermally induced moments due to the additional temperature at the bottom half of the cross section caused by the linear gradient.

DISCUSSION OF RESULTS

Results of Advanced Analyses

The structural members in compartment 5A were subjected to the full fire time-temperature curve. This resulted in failure of the internal gravity W12×58 column, as shown in Figure 10(b). This failure did not occur until the column reached 544°C at 95 min. Figure 10(a) shows the deflected shape of the structure at 60 min. At this time, the floor framing had deflected approximately 12 in., but no significant damage had occurred. The member demands that were determined from the ABAQUS model at 60 min will be summarized in order to compare results from the advanced and simple methods of analysis.

The compartment fires in 5B (exterior) and 5C (interior) also resulted in gravity column buckling at 95 min. The deformed shapes are shown in Figure 11(a) and 11(b) for compartment 5B and 5C, respectively. In compartment 5B, two of the gravity columns buckled, resulting in partial collapse of the structure. The compartment 5C fire resulted in buckling of all four gravity columns, which eventually led to complete collapse of the structure. Figure 11(b) shows a snapshot of the deformed shape prior to complete collapse. In both fire scenarios, the structure was able to withstand the fire until 95 min, which is beyond the 1-hr fire-resistance rating of the structure. The comparison of member demands in ABAQUS versus SAP2000 is provided in the Appendix of this paper.

Results of Simple Analyses

Axial Demands

Table 7 summarizes the axial demands for beams and columns computed in the SAP2000 models for each of the three aforementioned load cases (Cases 1–3). These demands were determined for compartment fires at 5A, 5B, and 5C. For brevity, results from fire 5A are described below, and fire 5B and 5C results are provided in the appendix of this paper. "CL" indicates beams along the column line, while "INF" indicates infill beams. "E" stands for edge column, and "C" means a corner column.

Case 1 does not include temperature effects, so the beams experience negligible axial loads and the columns have axial loads due only to gravity loads. Case 2 introduces member temperatures and the coefficient of thermal expansion. This causes axial loads in the beams. Note that the axial load of the W14×22 infill beams (not along the column lines) is minimal at only 5 kips because it frames into a girder that provides minimal restraint against expansion. This is in contrast to the W14×22 beams along the column lines that experience 45 kips of axial load due to the restraint provided by the column supports. Case 2 also tends to cause an increase in axial load for the moment frame columns. The gravity columns, however, do not experience any increase in axial loading due to temperature. This is because the members framing into the gravity columns are all modeled with idealized, pinned end conditions that do not restrain

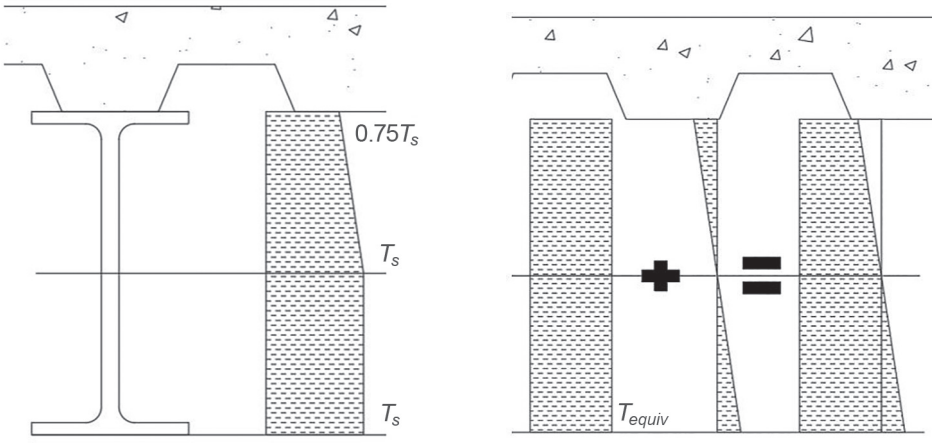

(a) Simple method *(b) SAP2000*

Fig. 9. Thermal gradient across composite beam section.

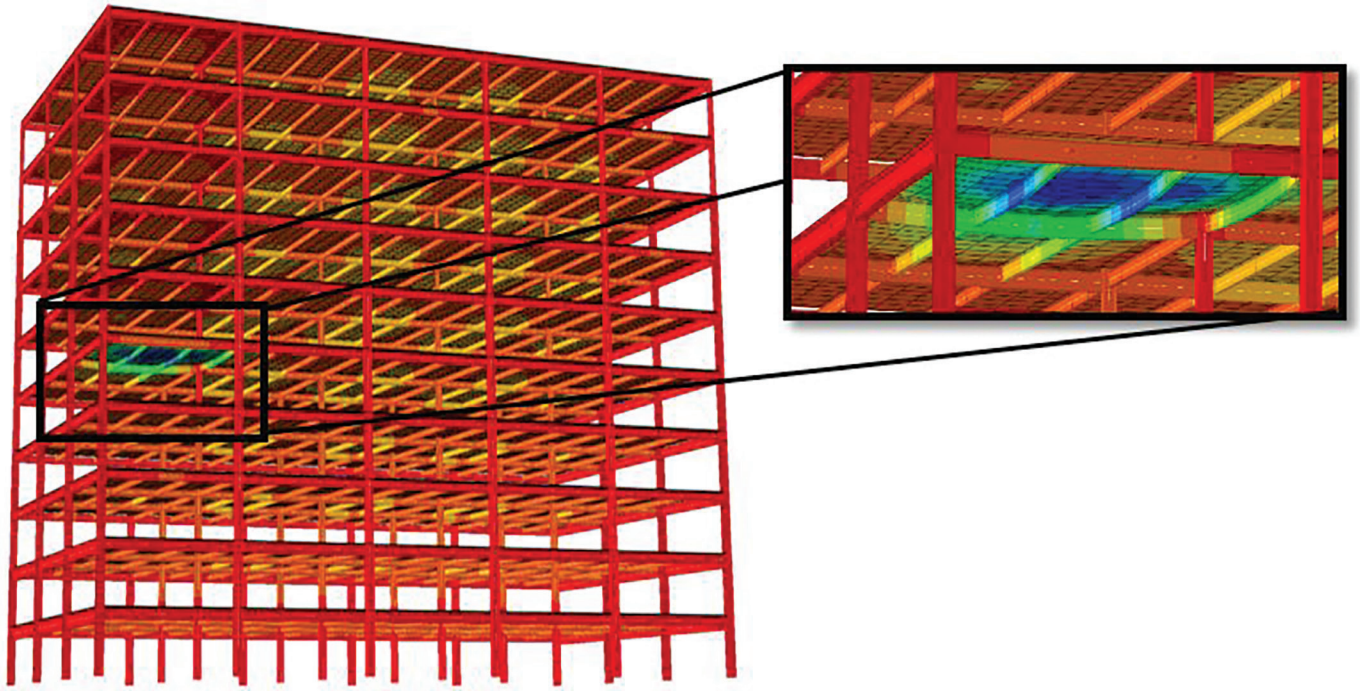

(a) At 60 minutes

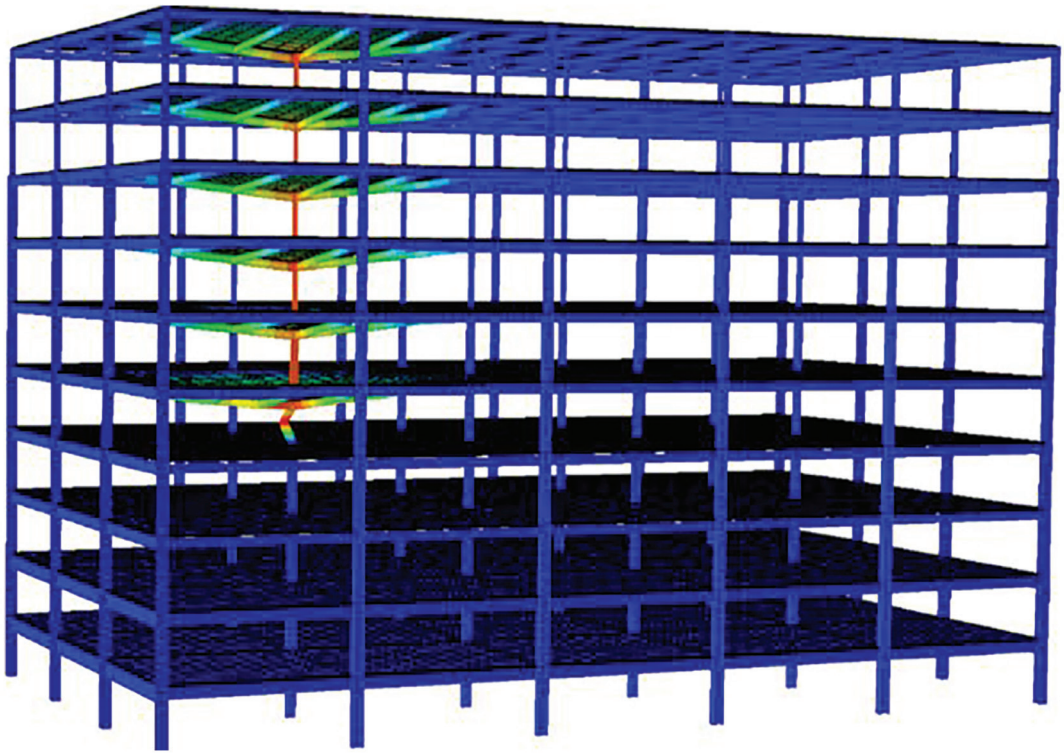

(b) At end of fire

Fig. 10. Deformed shape due to fire in compartment 5A.

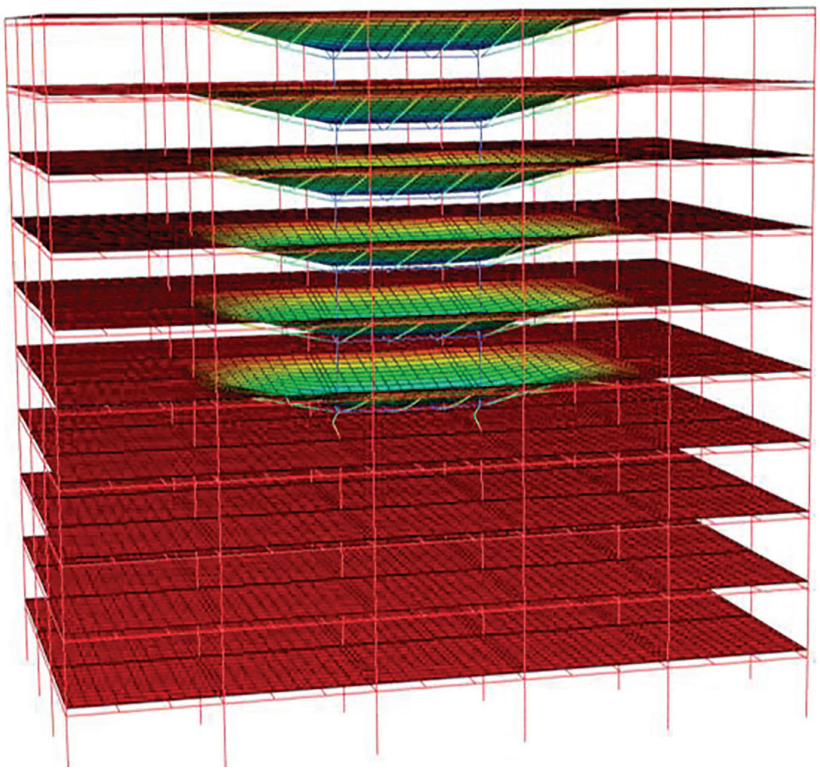

(a) Compartment 5B

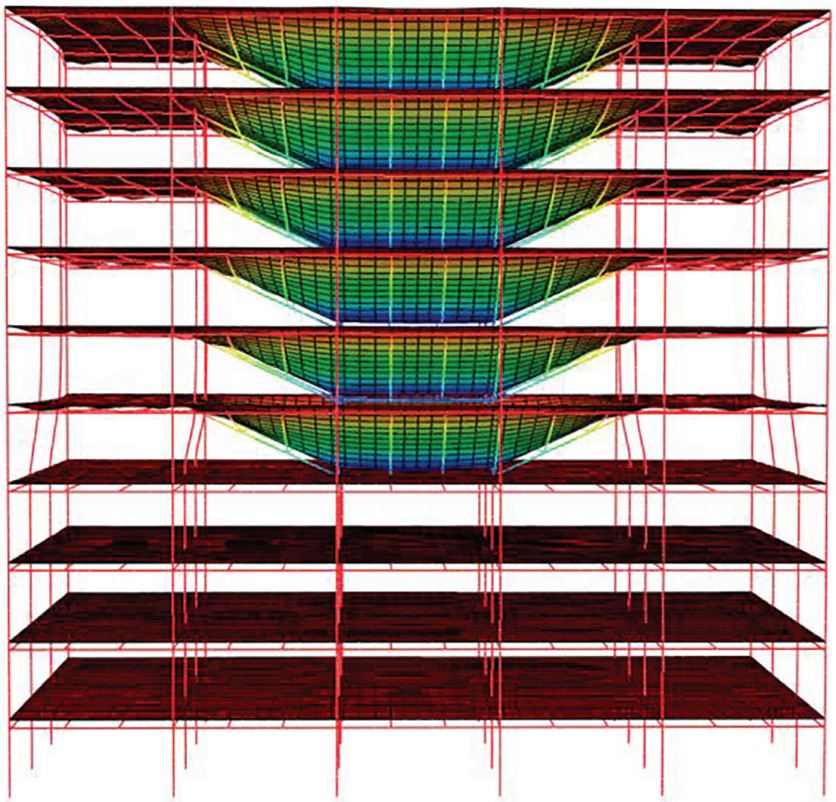

(b) Compartment 5C

Fig. 11. Deformed shape due to fire.

Table 7. Member Axial Demands Using the Simple Method: 5A				
	Member Size	**Case 1, kips**	**Case 2, kips**	**Case 3, kips**
Beams	W14×22 (CL)	0	45	36
	W14×22 (INF)	0	5	1
	W18×35	0	84	68
	W18×60	0	93	76
	W21×93	0	210	170
Columns	W12×58	404	404	404
	W14×99	232	278	271
	W14×109 (E)	212	292	288
	W14×109 (C)	103	61	67

Table 8. Member Flexural Demands: 5A							
	Member Size	**Case 1, kip-ft**		**Case 2, kip-ft**		**Case 3, kip-ft**	
		M_x	M_y	M_x	M_y	M_x	M_y
Beams	W14×22 (CL)	69	—	84	—	101	—
	W14×22 (INF)	69	—	68	—	69	—
	W18×35	186	—	211	—	228	—
	W18×60	95	—	375	—	243	—
	W21×93	55	—	403	—	253	—
Columns	W12×58	0	—	89	41	58	26
	W14×99	24	—	186	192	96	155
	W14×109 (E)	23	—	344	334	191	228
	W14×109 (C)	28	1	866	344	626	277

these columns from experiencing thermal expansion. The gravity connections, in reality, provide some amount of rotational restraint. This restraint is relatively minor, however, and can be ignored in the simple method of analysis for typical buildings. The only other scenario where Case 2 does not cause an increase in column axial load is for the corner column in compartment 5A; this column actually experiences a reduction in axial loading due to the moment connection at column line B-4 and the pinned connection at column line A-4.

Case 3 incorporates a reduced modulus of elasticity, which results in a reduction in axial loading of the members. This is explained by Equation 2, which shows that axial load due to thermal expansion is a function of the modulus of elasticity of the member.

Flexural Demands

Table 8 provides the resulting flexural demands from the SAP2000 model for compartment fires at 5A for each of the three model cases. The flexural beam demands are the result of gravity loading and thermal gradient. The beams and girders along the column lines experience higher demands than the infill beams due to increased restraint at these locations. Flexural demands are also very high in the moment frame columns and beams due to the elevated temperatures.

Axial Member Design Strength

AISC *Specification* Chapter E is used to calculate the design strength of compression members. In lieu of Equation E3-2, however, the following flexural buckling equation should be used (Appendix 4, Equation A-4-2):

$$F_{cr}(T) = \left[0.42^{\sqrt{\frac{F_y(T)}{F_e(T)}}}\right] F_y(T) \tag{4}$$

The designer should consider using a modified slenderness (L/r) value in order to account for the rotational restraints provided by the cooler columns above and/or below the compartment fire. Consideration must be made,

Table 9. Member Axial Design Strength					
	Member Size	**A, in.^{2}**	**$\phi P_n = 0.9F_y(T)A$, kips**		
Beams	W14×22	6.49	126		
	W18×35	10.3	348		
	W18×60	17.6	530		
	W21×93	27.3	916		
	Member Size	**L_c/r**	**$F_e(T)$, ksi**	**$F_{cr}(T)$, ksi**	**ϕP_n, kips**
Columns (pinned-pinned)	W12×58	57.4	49.1	18.3	281
	W14×99	39.4	112	24.8	649
	W14×109	39.2	121	26.6	766
	Member Size	**L_c/r**	**$F_e(T)$, ksi**	**$F_{cr}(T)$, ksi**	**ϕP_n, kips**
Columns (rotational restraint)	W12×58	35.8	130	24.8	379
	W14×99	22.1	356	31.3	820
	W14×109	22.9	355	33.2	956

however, to evaluate the likelihood of multistory fires or vertically moving fires that would compromise this assumption of rotational restraints. If deemed applicable, the calculated column design strength can be significantly improved using the modified slenderness. The modified L/r value, referred to as L_c/r, is defined as:

$$\left(\frac{L_c}{r}\right)_T = \left(1 - \frac{T-32}{n3{,}600}\right)\left(\frac{L_c}{r}\right) - \left(\frac{35}{n3{,}600}\right)(T-32) \geq 0 \quad (5)$$

where T is the column temperature (°F). If the columns above and below are both cooler, $n = 1$, and $n = 2$ if either the columns above or below are cooler. This slenderness equation was calibrated for gravity columns and is provided in AISC *Specification* Commentary Equation C-A-4-9. It can also be used for moment frame columns, though this equation is overly conservative for moment frame columns due to the additional benefit of the restraint from the fixed beam to column connections.

Due to thermal expansion, beams may also experience significant compression. The beam can be considered fully braced along its top flange due to the presence of the composite slab, so flexural buckling equations need not be analyzed. Instead, the beam has the following axial nominal strength: $P_n = F_y(T)A$, where A is the cross-sectional area of the steel member. The same resistance factor, ϕ, is used for both ambient and elevated temperature conditions. Member axial design strengths are shown in Table 9.

Flexural Member Design Strength

All beams were designed as composite beams. Although the moment frame beams (W18×60 and W21×93) were initially designed as noncomposite members to resist lateral loads, it was presumed that enough studs are present to enable composite action under gravity and fire loading.

Composite Beams

The composite beams were designed assuming a constant temperature between the bottom flange and the mid-depth of the web with a 25% linear reduction from the mid-depth to the top flange, as shown in Figure 10. Appendix 4 allows two approaches for calculating the flexural strength of composite beams: (1) calculate the nominal flexural strength of the beam at ambient conditions and apply a retention factor, $r(T)$, per Table A-4.2.4 or (2) design using Chapter I with reduced yield stresses in the steel. Results from both approaches are in Table 10 and produce very comparable flexural strengths. The composite beams were designed for ambient conditions using ¾-in.-diameter studs and a minimum of 25% composite action. Lightweight concrete (110 lb/ft^3) with 3.5 ksi compressive strength was assumed for the slab on metal deck. The nominal flexural strengths were calculated using plastic stress distribution method from Section I1.2a of the *Specification*.

Noncomposite Members

The flexural strength of the columns was determined using the non-composite flexural equations from Appendix 4. These design equations for the nominal flexural strength of members at elevated temperatures pertain to the yielding and lateral-torsional buckling limit states. They apply only to laterally unbraced doubly symmetric members that do not have slender elements. This approach applies modified equations from AISC *Specification* Chapter F. The steel properties at elevated temperatures from Section 4.2.3b

Table 10. Composite Beam Flexural Strength					
Member Size	***r(T)***	**Number of Studs, *n***	**$\phi M_n = 0.90M_n$, kip-ft**	**Approach 1: $\phi M_n(T) = 0.90r(T)M_n$, kip-ft**	**Approach 2: $\phi M_n(T) = 0.90M_n(T)$, kip-ft**
W14×22	0.55	20	231	127	125
W18×35	0.60	44	490	294	304
W18×60	0.72	26	664	478	450
W21×93	0.73	22	1026	750	750

Table 11. Column Flexural Strength, ϕM_n			
	Member Size	**$\phi M_{n,x}$, kip-ft**	**$\phi M_{n,y}$, kip-ft**
Column	W14×99	548	265
	W14×109	651	314
	W12×58	260	98

replace the ambient properties in Chapter F. When the unbraced length, L_b, of the member falls within the inelastic lateral-torsional buckling range [i.e., when $L_b < L_r(T)$, where $L_r(T)$ is the limiting unbraced length for inelastic lateral-torsional buckling], the nominal flexural strength can be calculated using Appendix 4, Equation A-4-3:

$$M_n(T) = C_b\left\{M_r(T) + \left[M_p(T) - M_r(T)\right]\left[1 - \frac{L_b}{L_r(T)}\right]^{c_x}\right\} \leq M_p(T) \quad (6)$$

where C_b is the lateral-torsional buckling modification factor. The other terms are defined as:

$$M_r(T) = S_x F_L(T) \quad (7)$$

$$F_L(T) = F_y(k_p - 0.3k_y) \quad (8)$$

$$M_p(T) = Z_x F_y(T) \quad (9)$$

$$c_x = 0.6 + \frac{T}{250} \leq 3.0 \text{ where } T \text{ is in °C} \quad (10)$$

and where S_x and Z_x are the elastic and plastic section moduli taken about the x-axis, respectively; k_p and k_y are retention factors for material properties at elevated temperatures and determined from AISC *Specification* Appendix 4, Table 4.2.1.

Table 11 provides the flexural strengths of the columns for the governing limit state. Note that because the W14×99 has a noncompact flange, flange local buckling (FLB) should also be checked. However, there is not yet guidance in Appendix 4 on how to apply FLB to flexural members using the simple method of analysis, so FLB was not analyzed. The columns experience reverse curvature bending under fire loading; values of $C_b = 2.2$ and 2.16 were calculated for the moment frame and gravity columns, respectively, using AISC *Specification* Equation F1-1. Due to the high C_b factors, yielding controlled the flexural strength.

Combined Force Member Interaction

The beams and columns in compartment 5A were subjected to axial and flexural demands, which required beam-column analyses. Each member was analyzed for combined axial and flexural forces using AISC *Specification* Chapter H, which implements an interaction check in Equations H1-1a and H1-1b. These equations are conservative for biaxial bending; to achieve interaction values closer to unity, alternative approaches outlined in the commentary of the *Specification* can be used instead to evaluate member adequacy. Table 12 summarizes the loads and strengths, as well as the interaction for all members within the compartment. The highlighted members are inadequate designs according to Equations H1-1a and H1-1b; these include the gravity column and all three moment frame columns. Design of the beam members were found to be adequate using the simple method of analysis.

It is presumed that the high demands on the moment frame columns are due in large part to the simplified modeling assumptions in the SAP2000 model. The composite slab is not incorporated in the model, so the stiffness of the moment frame beams in the model is less than what would realistically be present. Because of this, the moment frame columns carry very large moments. Additionally, the

Table 12. Beam-Column Interaction Check									
		P_u, kips	ϕP_n, kips	$P_u/\phi P_n$	M_x, kip-ft	M_y, kip-ft	$\phi M_{n,x}$, kip-ft	$\phi M_{n,y}$, kip-ft	Interaction Check (H1–1a/b)
Beams	W14×22 (CL)	36	126	0.39	101	—	127	—	0.99
	W14×22 (INF)	1	126	0.03	69	—	127	—	0.55
	W18×35	68	348	0.22	228	—	304	—	0.85
	W18×60	76	530	0.18	243	—	450	—	0.61
	W21×93	170	916	0.22	253	—	750	—	0.43
Columns	W12×58*	404	379	1.07	58	26	260	98	1.50
	W14×99	271	820	0.34	96	155	462	247	1.04
	W14×109 (E)	288	956	0.32	191	228	561	314	1.21
	W14×109 (C)	67	956	0.06	626	277	561	314	1.88
* If using a reduced axial demand due to LLR, the interaction check is 1.35.									

Table 13. Member Axial Demand vs. Design Strength Summary for Simple Method (Model Case 3)						
	Demand, P_u, kips		Design Strength, ϕP_n, kips		$P_u/\phi P_n$	
Beams	W14×22 (CL)	36	126		0.29	
	W14×22 (INF)	1	126		0.01	
	W18×35	68	348		0.20	
	W18×60	76	530		0.14	
	W21×93	170	916		0.19	
	Member Size	5A	Pin-Pin	Rotational Restraint	Pin-Pin	Rotational Restraint
Columns	W12×58	404	281	379	1.44	1.07
	W14×99	271	649	820	0.42	0.33
	W14×109 (E)	288	766	956	0.38	0.30
	W14×109 (C)	67	766	956	0.09	0.07

columns were evaluated without live load reduction, which results in larger demands on the columns. The gravity framing connections were also modeled as idealized pins, which do not transfer any moments. In reality, these connections have some level of rotational restraint that could help to redistribute large forces due to elevated temperatures. Each of the previously mentioned limitations of the simple method make this method overly conservative for moment frame columns and, therefore, unfavorable relative to the prescriptive method.

Axial Demand vs. Design Strength

A comparison of axial demand versus design strength, provided in Table 13, shows adequate strength for the beams and moment frame columns, but inadequate strength for the W12×58 gravity column. Incorporating rotational restraint in the calculation of column design strength provides a much closer approximation to the demands than considering a pin-pin column; however, both approaches indicate column failure within 1 hr of the start of the design fire. However, the column was designed without live load reduction, which would have resulted in a demand less than the calculated design strength.

Comparison of Methods

Table 14 summarizes a comparison between member demands using the advanced method of analysis (ABAQUS, noted as ABQ) and the simple method (SAP2000, noted as

Table 14. Comparison of Member Demands Between Advanced and Simple Methods											
		Axial Load, kips		M_x, kip-ft		M_y, kip-ft		V_x, kips		V_y, kips	
	Member Size	ABQ	SAP	ABQ	SAP	ABQ	SAP	ABQ	SAP	ABQ	SAP
Beams	W14×22 (CL)	50	36	58	101	2	0	12	11	5	0
	W14×22 (INT)	9	1	55	69	3	0	7	11	3	0
	W18×35	110	68	107	228	5	0	41	23	7	0
	W18×60	85	76	268	243	16	—	27	23	4	3
	W21×93	157	170	399	253	17	—	15	14	5	3
Columns	W12×58	422	404	61	58	17	26	13	8	13	2
	W14×99	299	271	46	96	106	155	8	16	21	26
	W14×109 (E)	285	288	161	191	188	228	26	35	31	38
	W14×109 (C)	46	67	496	626	178	277	88	111	48	50

SAP). The highlighted portions show differences between the modeling approaches of more than 15% or 15 kips (or kip-ft). Shear demands and capacities were also considered in these analyses but have not been presented for brevity. However, the summarized comparison of shear demands is also given in Table 14. SAP2000 typically resulted in larger demands than ABAQUS, though this was not always the case. The comparison shows close agreement between the axial forces in the members but varied results for the moment demands. In the gravity beams, SAP2000 tended to result in larger midspan moments because the ends were modeled as idealized pins, whereas the ABAQUS model incorporated some rotational restraint at the connections. SAP2000 also resulted in much larger moment demands on the columns than what was determined from the advanced analysis. As mentioned previously, this is likely due to the fact that the composite slab is not modeled in SAP2000. If the composite slab model was included in the simple analysis, the deviations in the predicted results relative to the advanced method would likely be greatly minimized. However, the advantage of the simple method is its speed and ease of modeling. If the designer were to begin incorporating composite slab behavior and catenary action into their simple analyses, then perhaps it would be more logical to employ the advanced analysis method.

It should also be noted that the temperature gradients used in the simple and advanced models for composite beams are different. The simple method utilizes an approach that is generally more conservative by only considering a 25% reduction in temperature at the top flange. In the advanced method of analysis, the reductions in temperature along the beam depth are typically greater. The differences in demand due to these thermal gradient differences can certainly contribute to the differential in the results. However, there are many other differences that also contribute, such as connection behavior, slab continuity, etc.

CONCLUSIONS

This work provides a comparison of the prescriptive, simple, and advanced methods of analysis, articulated through use of a case study building. It also proposes an approach for determining demands in the simple method of analysis through 3D modeling of the steel structural members in SAP2000. Member demands from elevated temperatures in the simple method can be determined by applying member temperatures and incorporating the coefficient of thermal expansion and reduced stiffness properties for the heated members. Variations in member demands were observed between the simple and advanced methods. These demand differences are to be expected because the simple method is an elastic analysis that overpredicts forces and uses simplifying modeling assumptions (idealized connections, no composite slab, etc.). These demand differences were deemed reasonable. The prescriptive and advanced methods demonstrated adequate performance of the structure. The simple method, however, provided more conservative results with inadequate moment frame designs for the columns. When using the simple method for checking moment frame members, the approach was even more conservative than the prescriptive method and is not suggested for this type of framing system. The findings from this particular study are not intended to imply that the use of the simple method is overly conservative in most cases. Instead, the use of the simple method may be found to be particularly advantageous and time-saving when considering gravity framing systems or when analyzing specific portions of a building structure.

Future Needs

Code officials in the United States remain hesitant to allow alternative methods to the prescriptive method for design of structural members for fire conditions. Thus, it is imperative that the designer work closely with the building owner and code officials to select adequate acceptance criteria that is in accordance with the owners' wishes and building codes. Efforts are under way at a number of U.S. universities to incorporate structural design for fire conditions into the structural engineering curriculum in order to equip future structural engineers with the skills necessary to perform structural engineering analyses and design for fire.

Despite these efforts, additional research and guidance is still needed to assure safe structural designs for fire. While the simple method of analysis provides a basic approach to LRFD design for members subjected to fire, AISC *Specification* Appendix 4 requires additional guidance for checking additional limit states, particularly local buckling states as well as compressive limits states other than flexural buckling. There is also a need for more guidance on how to consider connections in the simple and advanced methods of analysis. Additionally, thermal calculations are sensitive to the temperature-dependent SFRM properties. It is, therefore, crucial to establish reliable temperature-dependent SFRM material properties. Finally, more guidance is needed to assist designers in selecting appropriate design-basis fires. General acceptance of a standard fire curve for simple and advanced methods of analysis would assist in removing ambiguity about fire load characterization.

REFERENCES

ABAQUS (2016), Simulia, Dassault Systemes, Boston, Mass.

Agarwal, A. (2011), "Stability Behavior of Steel Building Structures in Fire Conditions," Doctoral Dissertation, School of Civil Engineering, Purdue University, West Lafayette, Ind.

Agarwal, A., Choe, L., and Varma, A.H. (2014), "Fire Design of Steel Columns: Effects of Thermal Gradients," *Journal of Constructional Steel Research*, Vol. 93, pp. 107–118.

Agarwal, A. and Varma, A.H. (2014), "Fire Induced Progressive Collapse of Steel Building Structures: The Role of Interior Gravity Columns," *Engineering Structures*, Vol. 58, pp. 129–140.

AISC (2016a), *Code of Standard Practice for Steel Buildings and Bridges*, ANSI/AISC 306-16, American Institute of Steel Construction, Chicago, Ill.

AISC (2016b), *Specification for Structural Steel Buildings*, ANSI/AISC 360-16, American Institute of Steel Construction, Chicago, Ill.

ASCE (2016), *Minimum Design Loads for Buildings and Other Structures*, ASCE/SEI 7-16, American Society of Civil Engineers, Reston, Va.

ASTM (2015), *Standard Test Methods for Fire Tests of Building Construction and Materials*, ASTM E119-15, ASTM International, West Conshohocken, Pa.

Carino, N.J., Starnes, M.A., Gross, J.L., Yang, J.C., Kukuck, S., Prasad, K.R., and Bukowski, R.W. (2005), "Federal Building and Fire Safety Investigation of the World Trade Center Disaster: Passive Fire Protection," NIST NCSTAR 1-6A, National Institute of Standards and Technology, Gaithersburg, Md, September.

Cedeno, G., Varma, A.H., and Gore, J. (2008), "Predicting the Standard Fire Behavior of Composite Steel Beams," in *Composite Construction in Steel and Concrete VI*, Engineering Conferences International, Colorado, pp. 642–656, ASCE, Reston, Va. http://dx.doi.org/10.1061/41142(396)53

Choe, L., Agarwal, A., and Varma, A.H. (2016), "Steel Columns Subjected to Thermal Gradients from Fire Loading: Experimental Evaluation," *Journal of Structural Engineering*, Vol. 142, No. 7.

CSI (2018), *SAP2000: Integrated Software for Structural Analysis and Design*, Computers and Structures, Inc., Berkeley, Calif.

ECCS Technical Committee 3 (1995), *Fire Resistance of Steel Structures*, ECCS Publication No. 89, European Convention for Constructional Steelwork, Brussels, Belgium.

ECCS Technical Committee 3 (2001), *Model Code on Fire Engineering*, ECCS Publication No. 111, European Convention for Constructional Steelwork, Brussels, Belgium.

CEN (2002), *Eurocode 1: Actions on Structures, Part 1-2: General Actions—Actions on Structures Exposed to Fire*, EN1991-1-2, European Committee for Standardization, Brussels, Belgium.

Fischer, E.C., Chicchi, R., and Choe, L. (2021), "Review of Research on the Fire Behavior of Simple Shear Connections," *Fire Technology*, Vol. 57, pp. 1,519-1,540.

Fischer, E.C., Varma, A.H., and Agarwal, A. (2019), "Performance-Based Structural Fire Engineering of Steel Building Structures: Design-Basis Compartment Fires," *Journal of Structural Engineering*, Vol. 145, No. 9.

Gernay, T. and Khorasani, N.E. (2020), "Recommendations for Performance-Based Fire Design of Composite Steel Buildings Using Computational Analysis," *Journal of Constructional Steel Research*, Vol. 166.

ICC (2018), *International Building Code*, IBC 2018, International Code Council, Falls Church, Va.

ISO (2015), *Fire Resistance Tests—Elements of Building Construction—Part 1: General Requirements*, ISO 834-1:1999, International Organization for Standardization, Geneva, Switzerland.

Khorasani, N.E., Gernay, T., and Fang, C. (2019), "Parametric Study for Performance-Based Fire Design of US Prototype Composite Floor Systems," *Journal of Structural Engineering*, ASCE, Vol. 145, No. 5.

Kodur, V.K.R., and Shakya, A.M. (2013), "Effect of Temperature on Thermal Properties of Spray Applied Fire Resistive Material," *Fire Safety Journal*, Vol. 61, pp. 314–323.

Main, J.A. and Sadek, F. (2013), "Robustness of Steel Gravity Frame Systems with Single-Plate Shear Connections," NIST Technical Note 1749, National Institute of Standards and Technology, Gaithersburg, Md. http://dx.doi.org/10.6028/NIST.TN.1749

NFPA (2020), *Standard for Determination of Fire Loads for Use in Structural Fire Protection Design*, NFPA 557, National Fire Protection Association, Quincy, Mass.

NIST (2013), *Fire Dynamics Simulator Users Guide*, 6th Ed., National Institute of Standards and Technology, Gaithersburg, Md. http://fire.nist.gov/fds/

Ruddy, J.L., Mario, J.P., Ioannides, S.A., and Alfawakhiri, F. (2003), *Fire Resistance of Structural Steel Framing*, AISC Design Guide 19, American Institute of Steel Construction, Chicago, Ill.

Sarraj, M. (2007), "The Behaviour of Steel Fin Plate Connections in Fire," Doctoral Dissertation, Department of Civil and Structural Engineering, The University of Sheffield, Sheffield, UK.

Takagi, J. and Deierlein, G.G. (2007), "Collapse Performance Assessment of Steel-Framed Buildings under Fires," Report No. 163, The John A. Blume Earthquake Engineering Center, Stanford University, Stanford, Calif.

UL (2018), "UL Online Certifications Directory: Fire-Resistance Ratings—ANSI/UL263." http://database.ul.com/

Yang, K.C., Chen, S.J., and Ho, M.C. (2009), "Behavior of Beam-to-Column Moment Connections under Fire Load," *Journal of Constructional Steel Research*, Vol. 65, No. 7, pp. 1,520–1,527.

APPENDIX

5B AND 5C ANALYSES

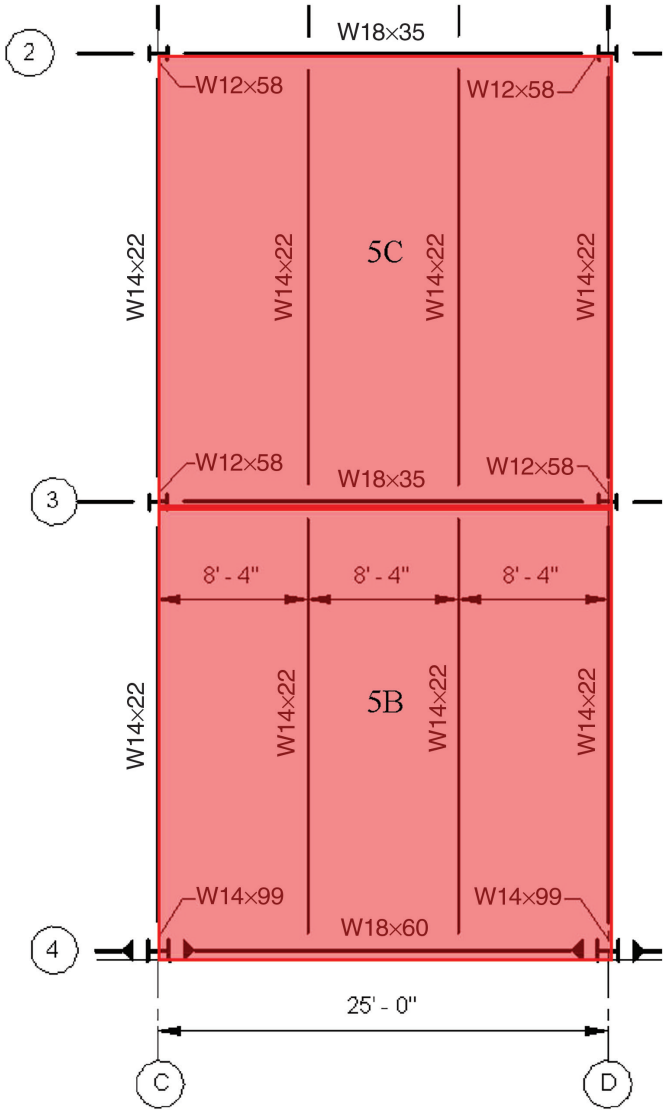

Table A.1. Member Axial Demands Using the Simple Method							
		5B			5C		
	Member Size	Case 1, kips	Case 2, kips	Case 3, kips	Case 1, kips	Case 2, kips	Case 3, kips
Beams	W14×22 (column line)	0	46	**37**	0	47	**40**
	W14×22 (infill)	0	4	**3**	0	3	**2**
	W18×35	0	112	**94**	0	111	**94**
	W18×60	0	250	**213**	—	—	**—**
	W21×93	—	—	**—**	—	—	**—**
Columns	W12×58	404	404	**404**	404	404	**404**
	W14×99	209	250	**248**	—	—	**—**
	W14×109 (E)	—	—	**—**	—	—	**—**
	W14×109 (C)	—	—	**—**	—	—	**—**

Table A.2. Member Axial Demand vs. Design Strength Summary					
		Demand, kips		Design Strength, kips	
	Member Size	5B	5C		
Beams	W14×22 (column line)	37	62	126	
	W14×22 (infill)	3	3	126	
	W18×35	94	81	348	
	W18×60	213	—	530	
	W21×93	—	—	916	
	Member Size	**5B**	**5C**	**Pin-Pin**	**Rotational Restraint**
Columns	W12×58	404	404	281	379
	W14×99	248	—	649	820

Table A.3. Member Flexural Demands: 5B							
	Member Size	Case 1, kip-ft		Case 2, kip-ft		Case 3, kip-ft	
		M_x	M_y	M_x	M_y	$\boldsymbol{M_x}$	$\boldsymbol{M_y}$
Beams	W14×22 (CL)	69	—	89	—	112	—
	W14×22 (INT)	69	—	68	—	68	—
	W18×35	186	6	215	5	248	4
	W18×60	67	—	267	18	164	11
Columns	W12×58	5	—	190	46	135	29
	W14×99	14	4	448	163	285	138

Table A.4. Member Flexural Demands: 5C							
	Member Size	Case 1, kip-ft		Case 2, kip-ft		Case 3, kip-ft	
		M_x	M_y	M_x	M_y	$\boldsymbol{M_x}$	$\boldsymbol{M_y}$
Beams	W14×22 (CL)	69	—	89	—	106	—
	W14×22 (INT)	69	—	68	—	67	—
	W18×35	186	—	224	2	248	1
Columns	W12×58	6	—	190	42	135	30

Table A.5. Member Demands Comparison (ABQ = ABAQUS Results, SAP = SAP2000 Results): 5B											
		Axial Load, kips		M_x, kip-ft		M_y, kip-ft		V_x, kips		V_y, kips	
	Member Size	ABQ	SAP	ABQ	SAP	ABQ	SAP	ABQ	SAP	ABQ	SAP
Beams	W14×22 (CL)	49	37	38	112	4	—	13	12	4	0
	W14×22 (INT)	14	3	27	68	2	—	11	11	2	0
	W18×35	115	94	103	248	4	4	24	23	3	1
	W18×60	276	213	76	164	5	11	16	12	5	4
Columns	W12×58	422	404	72	135	14	29	14	16	4	2
	W14×99	261	248	194	285	116	138	37	41	21	19

Table A.6. Member Demands Comparison (ABQ = ABAQUS Results, SAP = SAP2000 Results): 5C											
	Member Size	Axial Load, kips		M_x, kip-ft		M_y, kip-ft		V_x, kips		V_y, kips	
		ABQ	SAP	ABQ	SAP	ABQ	SAP	ABQ	SAP	ABQ	SAP
Beams	W14×22 (CL)	55	40	39	106	1	—	11	11	4	0
	W14×22 (INT)	29	2	31	67	1	—	12	11	4	0
	W18×35	124	94	108	248	4	1	24	21	3	0
Columns	W12×58	420	404	69	135	21	30	14	16	6	3

Table A.7. Interaction Checks: 5B									
		P_u, kips	ϕP_n, kips	$P_u/\phi P_n$	M_x, kip-ft	M_y, kip-ft	$\phi M_{n,x}$, kip-ft	$\phi M_{n,y}$, kip-ft	Interaction Check (H1–1a/b)
Beams	W14×22 (CL)	37	126	0.29	112	—	127	—	1.08
	W14×22 (INF)	3	126	0.02	68	—	127	—	0.55
	W18×35	94	348	0.27	248	—	304	—	1.0
	W18×60	213	530	0.40	164	11	450	—	0.91
Columns	W12×58	404	379	1.07	135	29	260	112	1.76
	W14×99	248	820	0.30	285	138	462	247	1.35

Table A.8. Interaction Checks: 5C									
		P_u, kips	ϕP_n, kips	$P_u/\phi P_n$	M_x, kip-ft	M_y, kip-ft	$\phi M_{n,x}$, kip-ft	$\phi M_{n,y}$, kip-ft	Interaction Check (H1–1a/b)
Beams	W14×22 (CL)	40	126	0.32	106	—	127	—	1.06
	W14×22 (INF)	2	126	0.02	67	—	127	—	0.54
	W18×35	94	348	0.27	248	—	304	—	0.70
Columns	W12×58	404	379	1.07	135	0	228	112	1.77